Journal of
Materials Chemistry C

PAPER

View Article Online
View Journal | View Issue

Open Access Article. Published on 02 September 2015. Downloaded on 11/7/2025 4:41:37 AM.
This article is licensed under a Creative Commons Attribution 3.0 Unported Licence.

Cite this: J. Mater. Chem. C, 2015, 3, 9664

Received 16th July 2015,
Accepted 25th August 2015

DOI: 10.1039/c5tc02162f

www.rsc.org/MaterialsC

High brightness deep blue/violet fluorescent polymer light-emitting diodes (PLEDs)†

Javan H. Cook,[a] José Santos,[b] Hameed A. Al-Attar,[a] Martin R. Bryce*[b] and Andrew P. Monkman*[a]

Two new deep blue/violet emitting alternating co-polymers, comprising readily-available carbazole (C) and fluorene (F) monomer units, have been synthesised and shown to produce extremely bright solution-processed polymer light-emitting diodes (PLEDs) with the structure ITO/PEDOT:PSS/polymer/TPBi/LiF/Al. The *para*-conjugated polymer, **CF1**, gave PLED devices with external quantum efficiency (EQE) values of $\eta_{ext,max}$ 1.4%, L_{max} of 565 cd m^{-2} with CIE$_{x,y}$ (0.16, 0.07). The EQE was raised to $\eta_{ext,max}$ 2.1%, after the addition of a TAPC hole injection layer. For the isomeric *meta*-conjugated polymer, **CF2**, values of $\eta_{ext,max}$ 0.35%, L_{max} of 16 cd m^{-2} with CIE$_{x,y}$ (0.18, 0.12) were obtained. The λ^{EL}_{max} was 409 nm for both the **CF1** and **CF2** devices. The **CF1** devices also possess low turn-on and low operating voltages for devices of such high brightness. Moreover, the **CF1** emission is very stable from 10 cd m^{-2} up to peak brightness, with only a negligible shift in CIE coordinates. The combination of a simple co-polymer structure synthesised using readily-available monomer units, and high brightness and good colour stability from a simple device architecture, makes **CF1** suitable for a wide range of applications requiring deep blue/violet emission.

1. Introduction

Organic light emitting devices (OLEDs) are a rapidly advancing technology due to their applications in full-colour flat-panel displays[1–4] and energy-saving solid-state lighting,[5–7] with numerous potential benefits over their inorganic competitors. These benefits include lower power consumption, faster response times, larger viewing angles, smaller sizes and greater ranges of colour and contrast, along with being cheap and quick to produce. OLEDs typically comprise multilayer structures which can give very bright and efficient devices when an emitter layer in sandwiched between additional layers that facilitate hole-transport and electron-transport. However, these multilayer devices have practical limitations as their fabrication is complicated by the need for sequential layer-by-layer deposition procedures. Furthermore, exciplex formation can occur at the organic–organic interfaces,[8,9] which can be detrimental for efficient and stable emission – especially in the blue spectral region.[10,11]

OLEDs which emit from the deep blue/violet region of the spectrum, especially with Commission Internationale de l'Eclairage (CIE) coordinates that match the National Television System Committee (NTSC) standard blue CIE$_{x,y}$ (0.14, 0.08) have been the subject of increased investigation to meet the demands of high quality displays.[12–21] Maximum external quantum efficiencies (EQEs) as high as 3–6% for emission peaks in the range 400–480 nm have been achieved for a range of small molecule based devices through rational molecular design.[12,21] However, efficient deep blue polymeric emitters in simple device architectures remain under-developed.[11,21] Polymeric systems which possess good solubility in organic solvents offer the advantages of rapid industrial-scale polymer LED (PLED) fabrication by solution processing techniques, such as ink-jet printing, spin-coating and roll-to-roll processing.[22] The key challenge in the molecular design of saturated blue emitting polymers is that backbone conjugation should be restricted to short (oligomer) segments, while the charge carrier transport capabilities of the polymer must be retained.[23]

Poly(9,9-dialkylfluorene-2,7-diyl) derivatives are widely used as blue/deep blue emitting polymers because of their high charge-carrier mobilities, good thermal and electrochemical stability, high photoluminescence quantum yields (PLQY), and versatile chemical modification.[24] Specific examples include: poly(3,6-silafluorene-*co*-2,7-fluorene),[25] poly(fluorene-*co*-thiophene) host–guest systems[26] and spiro-polyfluorenes.[27] Incorporation of tetrafluoro-*p*-phenylene units into a polyfluorene backbone affords PLEDs with EQEs as high as 5% with CIE coordinates of (0.16, 0.05).[28] It has recently been shown that the

[a] Department of Physics, Durham University, Durham, DH1 3LE, UK. E-mail: a.p.monkman@durham.ac.uk
[b] Department of Chemistry, Durham University, Durham, DH1 3LE, UK. E-mail: m.r.bryce@durham.ac.uk

† Electronic supplementary information (ESI) available: Synthesis and characterisation of **CF1** and **CF2**; absorption spectra; CIE diagrams. See DOI: 10.1039/c5tc02162f

This journal is © The Royal Society of Chemistry 2015

Open Access Article. Published on 02 September 2015. Downloaded on 11/7/2025 4:41:37 AM.
This article is licensed under a Creative Commons Attribution 3.0 Unported Licence.

attachment of bulky side chains to a polyfluorene backbone increases intrachain torsion angles and isolates minimal conjugated segments.[29–31] In an alternative approach, 9,9-diphenylfluorene units serve to disrupt conjugation in the polymer backbone leading to PLEDs with EQE values of $\eta_{ext,max}$ 3.9%, L_{max} of 274 cd m^{-2} with CIE$_{x,y}$ coordinates (0.17, 0.07).[32] It is also established that *meta*-linked aromatic units in the backbone can blue shift emission by reducing the effective conjugation length.[33–35] Sergent *et al.* have recently synthesised regiorandom fluorene–carbazole copolymers [with emphasis on different length alkyl chains at the fluorene C(9) position]. Very preliminary electroluminescence data showed blue emission (EQE 1.32%; CIE$_{x,y}$ 0.16; 0.11).[36]

The aim of the present work is to study new readily-available polymers which yield efficient deep blue/violet PLEDs. This has been achieved in two new high triplet energy poly(carbazole-*alt*-fluorene) co-polymers **CF1** and **CF2** which function as both the charge carrier transporters and the fluorescent emitters simultaneously. In both polymers the carbazole unit (C) is linked through 3,6-positions, while the linkage to the fluorene unit (F) is varied (2,7 in **CF1** – *para*-conjugated; 3,6 in **CF2** – *meta*-conjugated) in order to modulate the conjugation along the backbone. The photophysics and PLED applications of these co-polymers are reported. In particular, **CF1** devices emit deep blue/violet light with remarkably high brightness (L_{max} of 565 cd m^{-2}) when the luminosity function is taken into account. The luminosity function shows the perception of brightness to different wavelengths of light, as observed by the human eye and is the function by which OLED emission is normalised. Because the luminosity function peaks at 555 nm, blue and red emission is reduced in comparison to green emission, so more emission is required for these colours to achieve the same brightness. This becomes more of a problem the further the emission is from 555 nm, making the high brightness of **CF1** at 409 nm especially notable.

2. Results and discussion

2.1. Polymer synthesis and characterisation

The synthesis of the alternating copolymers **CF1** and **CF2** (Fig. 1) was carried out under standard Suzuki-Miyaura co-polymerisation conditions[37] followed by end-capping, as described in the ESI.† The co-polymers were characterised by GPC-UV-Vis data using polystyrene standards: **CF1** M_w 31 000 Da, M_n 10 800; **CF2** M_w 21 000 Da, M_n 6051 Da. The thermal properties of the polymers were characterised by thermal gravimetric analysis (TGA) and differential scanning calorimetry (DSC) under a nitrogen atmosphere. The decomposition temperature (T_d), which corresponds to a weight loss of 5% at a heating rate of 10 °C min^{-1}, was 433 °C and 422 °C for **CF1** and **CF2**, respectively, demonstrating that the polymers have very good thermal stability. Glass transition temperatures (T_g) of 134 °C and 130 °C for **CF1** and **CF2** were determined by DSC during the second heating cycle. In addition, no exothermic crystallisation or endothermic melting peaks were observed over the range 40–200 °C, implying that the polymers should exhibit high morphological stability in a device. These data are typical of copolymers of 9,9-dialkylfluorenes[38] and represent increased thermal stability compared to poly(9,9-dialkylfluorene)s, due to the reduced number of alkyl chains in **CF1** and **CF2**.[39] In particular T_g is raised significantly compared to poly(9,9-dihexylfluorene) (T_g 83 °C)[40] showing that the *N*-hexylcarbazole units effectively suppress the dense packing and crystallisation of the polymer chains.[41]

2.2. Optical properties

The spectroscopic data for polymers **CF1** and **CF2** is summarised in Table 1. Their absorption spectra are shown in the ESI† and their photoluminescence spectra are shown in Fig. 2. The polymers are deep blue/violet emitters (λ_{max}^{PL} in thin films: 421 and 401 nm, respectively). They exhibit very little solvatochromism, in agreement with previous work on fluorene co-polymers;[29,30,32] the small changes observed can be explained by the different refractive index of the solvents.

From the photophysical data in Table 2 it can be observed that both **CF1** and **CF2** emissions peak at *ca.* 400 nm in solution with negligible solvent polarity effect (Table 2, Fig. 2a and b). Nevertheless, PL from thin films shows a different trend: while **CF1** (*para*-conjugated) shows the typical aggregation induced red-shift (20 nm) in its emission, **CF2**'s (*meta*-conjugated) λ_{max}^{PL} remains basically unaltered (Table 2 and Fig. 2c).

No significant difference is observed in the film PLQY for polymers **CF1** and **CF2**, with values of Φ_{PL} 0.20 and 0.17, respectively. The observed triplet level for **CF1** and **CF2** (E_T^{onset} 2.34 eV) corresponds well to the reported values for poly(9,9-dialkylfluorene)[42] and poly(*N*-alkylcarbazole) derivatives[43] (*ca.* 2.3 eV) and related polymers with limited backbone π-conjugation.[29,30,32]

2.3. PLED device fabrication and properties

Hybrid devices were fabricated with **CF1** or **CF2** as the spin-coated light-emitting polymer (LEP) layer with the structure: glass|ITO (150 nm)|PEDOT:PSS 1.5 (70 nm)|LEP (**CF1** or **CF2** 20 nm)|TPBi (20 nm)|LiF (1 nm)|Al (100 nm). For all of the devices, no other

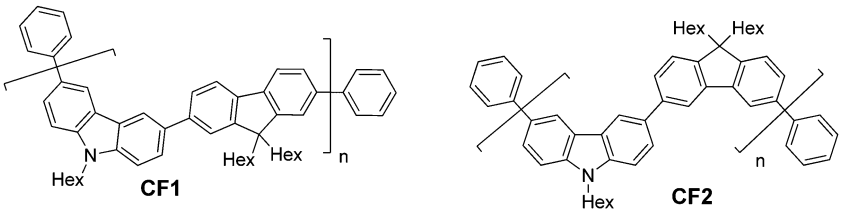

Fig. 1 Structures of the new deep blue/violet emitting carbazole-*alt*-fluorene copolymers studied in this work.

Open Access Article. Published on 02 September 2015. Downloaded on 11/7/2025 4:41:37 AM.
This article is licensed under a Creative Commons Attribution 3.0 Unported Licence.

Table 1 Photophysical data for the polymers **CF1** and **CF2**

Polymer	Solvent/film	λ_{max}^{abs}/nm	λ_{max}^{PL}/nm	PLQY, Φ_{PL} [a]	E_T^{onset} [b]/eV
CF1	Ethyl acetate	348	399		
	Cyclohexane	344	394		
	Film	350	421	0.20	2.34
CF2	Ethyl acetate	300	400		
	Cyclohexane	304	399		
	Film	287	401	0.17	2.34

[a] PLQY is the photoluminescence quantum yield. [b] E_T is the triplet energy determined for solid state samples at 16 K.

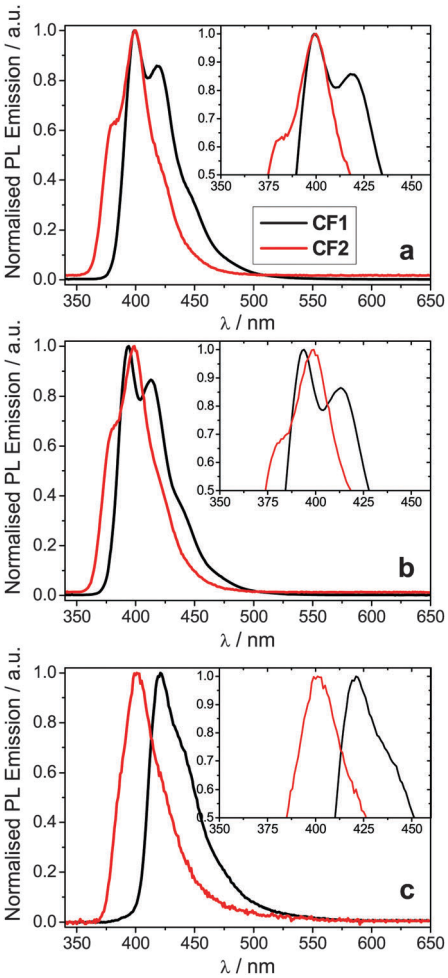

Fig. 2 Normalised PL emission spectra for polymers **CF1** and **CF2** (a) in ethyl acetate; (b) in cyclohexane; (c) in thin film. The insets show a magnification of the λ_{max} region.

dopants or transporters were added to the LEP layer. An evaporated layer of 1,3,5-tris(*N*-phenylbenzimidazole-2-yl)benzene (TPBi) was incorporated as a standard electron-injecting material to improve device performance (efficiency, brightness and turn-on voltage).[44] The thickness of the LEP layer was optimised for maximum device performance.

The device results are shown in Fig. 3 and 4. Devices containing **CF1** display deep blue/violet EL with λ_{max} of 409 nm and maximum EQE of 1.4% and CIE$_{x,y}$ coordinates [turn on (0.16, 0.07) and peak (0.16, 0.07)] exhibiting excellent stability under device operation. **CF2** also showed deep blue/violet emission, again with λ_{max} 409 nm, but with a substantially reduced EQE of 0.35% and less impressive colour coordinates [turn on (0.18, 0.12) and peak (0.20, 0.15)] with reduced stability. The CIE coordinates for **CF1** are considerably deeper in the blue than data recently reported for other fluorene–carbazole co-polymer PLEDs [(0.16, 0.11) and (0.18, 0.14)].[36] This excellent colour stability of the **CF1** emission is in contrast to most other deep blue polymers[32] for which there is a shift to less blue emission at maximum brightness (as seen here for **CF2**). CIE diagrams can be found in the ESI.† The results for **CF1** compare very favourably with pure PFO devices,[28] having a deeper blue λ_{max} (409 nm compared to 420 nm), superior CIE coordinates ((0.16, 0.07) compared to (0.16, 0.11)) and higher EQE and device efficiencies (1.10% and 0.51 cd A^{-1} compared to 0.56% and 0.20 cd A^{-1}). The emission is also deeper blue than reported recently in very preliminary EL data for regio-random fluorene–carbazole copolymers (CIE$_{x,y}$ 0.16; 0.11),[36] demonstrating the benefits of the well-defined alternating structure of **CF1**.

Polymer **CF1** produced an excellent maximum brightness of 565 cd m^{-2} for a device with these CIE coordinates. As stated in the introduction, this deep blue spectral region is heavily affected by the luminosity function (the eye sensitivity here is very low) making such a high value particularly notable. The low turn-on voltage (3.40 V) and low potential operating voltage makes this polymer well suited for a wide range of practical applications, including displays[1–4] and medical devices: for the latter "blue light therapy" has a range of beneficial effects.[45] **CF2** has a substantially reduced maximum brightness of 16 cd m^{-2}. Also, despite the emission showing a bluer onset compared to **CF1** and the same λ_{max} of 409 nm for both devices, the CIE coordinates of **CF2** are less blue than **CF1** due to broadened emission into the green region which skews the coordinates (Fig. 4).

The *meta*-linkage through the 3,6-positions of fluorene in **CF2** limits the backbone conjugation; this in turn reduces the

Table 2 Electroluminescent device data[a]

	V_{on} [b]/V	Brt/cd m^{-2}	EQE/%	Dev eff/cd A^{-1}	Brt$_{max}$/cd m^{-2}	EQE$_{max}$/%	Dev eff$_{max}$/cd A^{-1}	Lum$_{max}$/lm W^{-1}	CIE$_{x,y}$ [e]	CIE$_{x,y}$ [f]
CF1	3.40	232[c]	1.10[c]	0.51[c]	565 (492)[d]	1.4 (2.1)[d]	0.65	0.63	0.16, 0.07	0.16, 0.07
CF2	4.50	16[c]	0.05[c]	0.04[c]	16	0.35	0.25	0.99	0.18, 0.12	0.20, 0.15

[a] Device architecture: ITO/PEDOT:PSS/polymer/TPBi/LiF/Al. [b] V_{on} is the turn-on voltage, defined here as the voltage at which the device reaches a brightness of 10 cd m^{-2}. [c] A comparison current density of 10 mA cm^{-2} was selected. [d] Data in brackets are for devices with an additional TAPC layer between PEDOT:PSS and **CF1** (see text for details). [e] CIE coordinates at the turn-on voltage (10 cd m^{-2}). [f] CIE coordinates at the maximum brightness. CIE diagrams are shown in the ESI.

Open Access Article. Published on 02 September 2015. Downloaded on 11/7/2025 4:41:37 AM.
This article is licensed under a Creative Commons Attribution 3.0 Unported Licence.

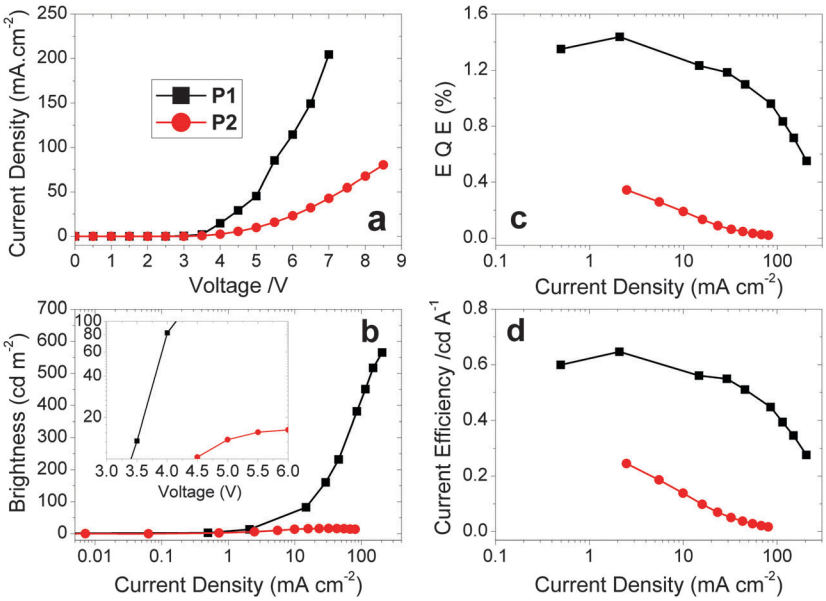

Fig. 3 Plots of (a) J–V curves. (b) Luminance *vs.* J. (c) EQE *vs.* J. (d) Device efficiency *vs.* J for the polymers **CF1** and **CF2**. Inset to (b) shows the low turn-on voltages for the two devices in a plot of luminance *vs.* V. The device structure is stated in Table 2, footnote *a*.

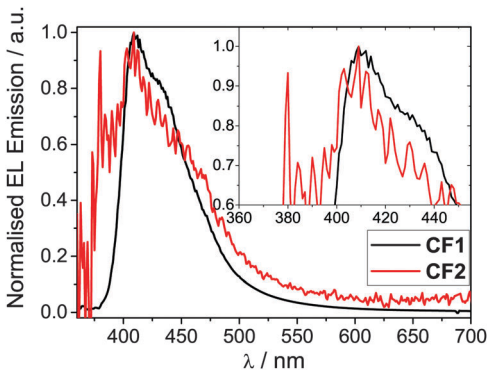

Fig. 4 Normalised EL emission spectra for polymers **CF1** and **CF2** devices. Inset shows a magnification of the λ_{max} region. The device structure is stated in Table 2, footnote *a*.

conductivity which explains the decrease in the current density passing through the **CF2** device, compared to **CF1**. This reduces both the maximum brightness and EQE of the **CF2** device, whilst causing no substantial blue shift in EL emission.

To further investigate **CF1**, devices were fabricated with an additional hole-injection and electron-blocking layer of 1,1-bis[(di-4-tolylamino)phenyl]cyclohexane (TAPC).[46] The primary purpose of this layer was to boost device efficiency by preventing electrons from reaching the anode and trapping them in the emissive layer, utilising TAPC's poor electron mobility. Two TAPC thickness were trialled to give the structure: glass|ITO (150 nm)|PEDOT:PSS HIL 1.5 (70 nm)|TAPC (60 nm or 90 nm)|LEP (20 nm)|TPBi (20 nm)|LiF (1 nm)|Al (100 nm). Whilst these TAPC thicknesses are both high relative to the LEP thickness, it was assumed that a portion would be washed away during deposition of the LEP layer leaving a more reasonable thickness behind that could be assessed by ellipsometry. The EQE was raised to $\eta_{ext,max}$ 2.1%. There was, however, a 25% increase in turn-on voltage and a 13% decrease in the maximum brightness. These were initially believed to be the result of increased device thickness and potential absorption by the TAPC layer, respectively. However, ellipsometry of the multilayer structures returns a combined thickness for the two layers between 19–20 nm. This indicates that the majority of the TAPC layer is removed when the LEP layer is deposited. Despite this, the observed changes in device properties fit with those expected for the addition of an electron blocking layer and so further investigation would be required to determine whether either a very thin film of TAPC remains, or whether the two layers have blended.

4. Conclusions

This work has addressed the synthesis, photophysical characterisation and device properties of two well-defined fluorene-*alt*-carbazole co-polymers **CF1** and **CF2** which are deep blue/violet emitters, with λ_{max}^{EL} 409 nm. The *para*-conjugated polymer, (**CF1**), with 2,7-linked fluorene units, is the most efficient emitter, giving PLED devices with external quantum efficiency (EQE) values of $\eta_{ext,max}$ 1.4%, L_{max} of 565 cd m^{-2} with CIE$_{x,y}$ (0.16, 0.07). The *meta*-conjugated polymer, **CF2**, with 3,6-linked fluorene units, gives analogous devices with $\eta_{ext,max}$ 0.35%, L_{max} of 16 cd m^{-2} with CIE$_{x,y}$ (0.18, 0.12). The emission of **CF1** devices shows excellent colour stability from 10 cd m^{-2} up to peak brightness, with essentially no shift in the CIE coordinates. The unique combination of a simple co-polymer structure that is based on cheap, readily-available monomer units, low turn-on voltage, excellent colour stability and high brightness in a simple PLED architecture makes **CF1** a very promising material for a wide range of applications requiring deep blue/violet emission.

Open Access Article. Published on 02 September 2015. Downloaded on 11/7/2025 4:41:37 AM.
This article is licensed under a Creative Commons Attribution 3.0 Unported Licence.

5. Experimental

5.1. Synthesis of polymers CF1 and CF2

The syntheses followed standard routes as reported in the ESI.†

5.2. Optical characterisation

Absorption spectra for solution and solid state samples were obtained using a Shimadzu UV-vis-NIR spectrophotometer whilst emission spectra were acquired using a Jobin-Yvon fluoromax spectrofluorimeter. The PLQY data was also obtained using the Jobin-Yvon fluoromax spectrofluorimeter, along with a small integrating sphere and a neutral density filter (optical density = 2).[47] The excitation wavelengths were determined from the maximum absorbance of the polymers as obtained from their absorption spectra. The triplet energies of solid state samples at 16 K were calculated using a gated luminescent measurement of the phosphorescence. Solutions were produced in ethyl acetate or cyclohexane, and the OD kept below 1.0. Solid state samples were drop-cast from a 1 : 1 mixture of 175 mg mL^{-1} zeonex and 0.5 mg mL^{-1} of the polymer, both in chlorobenzene, and had a maximum absorbance of 2.0 OD.

5.3. Device fabrication and characterisation

These devices featured an ITO anode (150 nm, 16 Ω^{-1}) commercially pre-coated on a glass substrate (24 mm × 24 mm). The substrates were cleaned with acetone, isopropanol and acetone sequentially in a sonic bath for a period of 9 min each. They were then exposed to low pressure plasma for a period of 3 min and treated with UV-ozone for a further 4 min. A hole-injection layer (HIL) of PEDOT:PSS of thickness 70 nm was deposited by spin coating and then baked on a hotplate at 200 °C for 3 min to remove any remaining moisture. The PEDOT:PSS used was the commercially available HIL 1.5 from Heraeus Precious Metals, Germany. Active layers of polymers **CF1** and **CF2** were prepared in a solution of chlorobenzene, with the concentration varied to produce layers of 60 nm thickness, and then spun on top of the PEDOT:PSS. The device was then annealed at 120 °C on a hotplate for 10 min to remove residual chlorobenzene. An electron injection layer (EIL) consisting of a 20 nm layer of 1,3,5-tris(*N*-phenylbenzimidazol-2-yl)benzene (TPBi) was thermally evaporated directly on top of the polymer layer. This was followed by a 1 nm thick lithium fluoride (LiF) cathode, which was thermally evaporated using a shadow mask to produce parallel strips perpendicular to the ITO anodes, forming four individually addressable pixels per substrate each of 5 mm × 4 mm area. The LiF was capped with a 100 nm thick layer of aluminium to protect it from oxidation. An evaporation pressure of the order of 10^{-6} mbar and a rate of approximately 0.1 nm s^{-1} was used for all of the evaporated produced layers. The devices were then encapsulated with DELO UV curable epoxy (Katiobond) and a 12 × 12 mm glass cover slide.

The devices were characterised in a calibrated Labsphere LMS-100 integrating sphere, connected to a USB 4000 CCD spectrometer supplied by a 30 μm UV/Vis fibre optic cable, under steady state conditions. Layer thicknesses were measured using a J. A. Woolam VASE Ellipsometer after having been spin coated onto Si/SiO_2 substrates. The non-uniformity of the organic layer thicknesses across the samples leads to a 5–10% error in device efficiencies: all measurements were averages from at least four devices.

Acknowledgements

The authors acknowledge the financial support of the Durham Energy Institute and EPSRC.

References

1 R. Mertens, *The OLED Handbook. A Guide to OLED Technology, Industry and Market*, 2014, www.oled-info.com/handbook.
2 A. C. Grimsdale, K. L. Chan, R. E. Martin, P. G. Jokisz and A. B. Holmes, *Chem. Rev.*, 2009, **109**, 897–1091.
3 K. Müllen and U. Scherf, *Organic Light-Emitting Devices*, Wiley-VCH, Weinheim, Germany, 2006.
4 Z. Li and H. Meng, *Organic Light-Emitting Materials and Devices*, CRC Press, Boca Raton, Florida, 2006.
5 K. T. Kamtekar, A. P. Monkman and M. R. Bryce, *Adv. Mater.*, 2010, **22**, 572–582.
6 S. Beaupré, P. L. T. Boudrealt and M. Leclerc, *Adv. Mater.*, 2010, **22**, E6–E27.
7 L. Ying, C.-L. Ho, H. Wu, Y. Cao and W.-Y. Wong, *Adv. Mater.*, 2014, **26**, 2459–2473.
8 Y. Shirota, *J. Mater. Chem.*, 2000, **10**, 1–25.
9 M. Castellani and D. Berner, *J. Appl. Phys.*, 2007, **102**, 024509.
10 M. Carvelli, A. van Reenen, R. A. J. Janssen, H. P. Loebl and R. Coehoorn, *Org. Electron.*, 2012, **13**, 2605–2614.
11 V. Jankus, C.-J. Chiang, F. Dias and A. P. Monkman, *Adv. Mater.*, 2013, **25**, 1455–1459.
12 X. Yang, X. Xu and G. Zhou, *J. Mater. Chem. C*, 2015, **3**, 913–944.
13 A. L. Fisher, K. E. Linton, K. T. Kamtekar, C. Pearson, M. R. Bryce and M. C. Petty, *Chem. Mater.*, 2011, **23**, 1640–1642.
14 X. J. Feng, S. F. Chen, Y. Ni, M. S. Wong, M. M. K. Lam, K. W. Cheah and G. Q. Lai, *Org. Electron.*, 2014, **15**, 57–64.
15 S. H. Jeong and J. Y. Lee, *J. Mater. Chem.*, 2011, **21**, 14604–14609.
16 S. Nau, N. Schulte, S. Winkler, J. Frisch, A. Vollmer, N. Koch, S. Sax and E. J. W. List, *Adv. Mater.*, 2013, **25**, 4420–4424.
17 Y.-H. Chung, L. Sheng, X. Xing, L. Zheng, M. Bian, Z. Chen, L. Xiao and Q. Gong, *J. Mater. Chem. C*, 2015, **3**, 913–944.
18 Y. Yang, P. Cohn, A. L. Dyer, S.-H. Eom, J. R. Reynolds, R. K. Castellano and J. Xue, *Chem. Mater.*, 2010, **22**, 3580–3582.
19 J. Ye, Z. Chen, M.-K. Fung, C. Zheng, X. Ou, X. Zhang, Y. Yuan and C.-S. Lee, *Chem. Mater.*, 2013, **25**, 2630–2637.
20 X. Zhan, N. Sun, Z. Wu, J. Tu, L. Yuan, X. Tang, Y. Xie, Q. Peng, Y. Dong, Q. Li, D. Ma and Z. Li, *Chem. Mater.*, 2015, **27**, 1847–1854.

 This journal is © The Royal Society of Chemistry 2015

Open Access Article. Published on 02 September 2015. Downloaded on 11/7/2025 4:41:37 AM.
This article is licensed under a Creative Commons Attribution 3.0 Unported Licence.

21 M. Zhu and C. Yang, *Chem. Soc. Rev.*, 2013, **42**, 4963–4976.
22 A. C. Arias, J. D. MacKenzie, I. McCulloch, J. Rivnay and A. Salleo, *Chem. Rev.*, 2010, **110**, 3–24.
23 D. Y. Kim, H. N. Cho and C. Y. Kim, *Prog. Polym. Sci.*, 2000, **25**, 1089–1139.
24 U. Scherf and E. J. W. List, *Adv. Mater.*, 2002, **14**, 477–487.
25 E. G. Wang, C. Li, Y. Q. Mo, Y. Zhang, G. Ma, W. Shi, J. B. Peng, W. Yang and Y. Cao, *J. Mater. Chem.*, 2006, **16**, 4133–4140.
26 G. Vamvounis, G. L. Schulz and S. Holdcroft, *Macromolecules*, 2004, **37**, 8897–8902.
27 C.-W. Huang, C.-L. Tsai, C.-Y. Liu, T.-H. Jen, N.-J. Yang and S.-A. Chen, *Macromolecules*, 2012, **45**, 1281–1287.
28 U. Giovanella, C. Botta, F. Galeotti, B. Vercelli, S. Battiato and M. Pasinbi, *J. Mater. Chem. C*, 2013, **1**, 5322–5329.
29 K. T. Kamtekar, H. L. Vaughan, B. P. Lyons, A. P. Monkman, S. U. Pandya and M. R. Bryce, *Macromolecules*, 2010, **43**, 4481–4488.
30 J. H. Cook, J. Santos, H. Li, H. A. Al-Attar, M. R. Bryce and A. P. Monkman, *J. Mater. Chem. C*, 2014, **2**, 5587–5592.
31 J. Liu, S. Hu, W. Zhao, Q. Zou, W. Luo, W. Yang, J. Peng and Y. Cao, *Macromol. Rapid Commun.*, 2010, **31**, 496–501.
32 J. Santos, J. H. Cook, H. A. Al-Attar, A. P. Monkman and M. R. Bryce, *J. Mater. Chem. C*, 2015, **3**, 2479–2483.
33 J. Ritchie, J. A. Crayston, J. P. J. Markham and I. D. W. Samuel, *J. Mater. Chem.*, 2006, **16**, 1651–1656.
34 P. Taranekar, M. Abdulbaki, R. Krishnamoorti, S. Phanichphant, P. Waenkaew, D. Patton, T. Fulghum and R. Advincula, *Macromolecules*, 2006, **39**, 3848–3854.
35 Z. L. Wu, Y. Xiong, J. H. Zou, L. Wang, J. C. Liu, Q. L. Chen, W. Yang, J. B. Peng and Y. Cao, *Adv. Mater.*, 2008, **20**, 2359–2364.
36 A. Sergent, G. Zucchi, R. B. Pansu, M. Chaigneau, B. Geffroy, D. Tondelier and M. Ephritikhine, *J. Mater. Chem. C*, 2013, **1**, 3207–3216. In Scheme 1 in this article, the structures are drawn with the carbazole units linked into the polymer chain through the 3,7-positions. Presumably this is an error as it is stated that the monomer used in the synthesis is 3,6-disubstituted carbazole.
37 (*a*) J. Murage, J. W. Eddy, J. R. Zimbalist, T. B. McIntyre, Z. R. Wagner and F. E. Goodson, *Macromolecules*, 2008, **41**, 7330–7338; (*b*) J. Sakamoto, M. Rehahn, G. Wegner and A. D. Schluter, *Macromol. Rapid Commun.*, 2009, **30**, 653–687.
38 L. Kinder, J. Kanicki, J. Swensen and P. Petroff, *Proceedings of SPIE Organic Field Effect Transistors II*, ed. C. D. Dimitrakopoulos and A. Dodabalapur, SPIE, Bellingham, WA, 2003, vol. 5217, pp. 35–42.
39 S. Jegadesan, S. Sindhu, R. C. Advincula and S. Valiyaveettil, *Langmuir*, 2006, **22**, 780–786.
40 K. L. Chan, S. E. Watkins, C. S. K. Mak, M. J. McKiernan, C. R. Towns, S. I. Pascu and A. B. Holmes, *Chem. Commun.*, 2005, 5766–5768.
41 Y. Zhu, K. M. Gibbons, A. P. Kulkarni and S. A. Jenekhe, *Macromolecules*, 2007, **40**, 804–813.
42 A. P. Monkman, H. D. Burrows, L. J. Hartwell, L. E. Horsburgh, I. Hamblett and S. Navaratnam, *Phys. Rev. Lett.*, 2001, **86**, 1358–1361.
43 K. Zhang, Y. Tao, C. Yang, H. You, Y. Zou, J. Qin and D. Ma, *Chem. Mater.*, 2008, **20**, 7324–7331.
44 J.-H. Jou, W.-B. Wang, S.-M. Shen, S. Kumar, I.-M. Lai, J.-J. Shyue, S. Lengvinaite, R. Zostautiene, J. V. Grazulevivius, S. Grigalevicius, S.-Z. Chen and C.-C. Wu, *J. Mater. Chem.*, 2011, **21**, 9546–9552.
45 (*a*) S. Vandersee, M. Beyer, J. Lademann and M. E. Darvin, *Oxid. Med. Cell. Longevity*, 2015, **2015**, 579675; (*b*) Y. Zhang, Y. Zhu, A. Gupta, Y. Huang, C. K. Murray, M. S. Vrahas, M. E. Sherwood, D. G. Baer, M. R. Hamblin and T. Dai, *J. Infect. Dis.*, 2014, **209**, 1963–1971.
46 G. Liaptsis and K. Meerholz, *Adv. Funct. Mater.*, 2013, **23**, 359–365.
47 L.-O. Palsson and A. P. Monkman, *Adv. Mater.*, 2002, **14**, 757–758.